

Effects of spatial variability of earthquake ground motion in cable-stayed bridges

Miguel P. Ferreira[†] and João H. Negrão[‡]

*Civil Engineering Department, University of Coimbra, Pinhal de Marrocos, Polo II,
3030-290 Coimbra, Portugal*

(Received July 20, 2005, Accepted February 27, 2006)

Abstract. Most codes of practice state that for large in-plane structures it is necessary to account for the spatial variability of earthquake ground motion. There are essentially three effects that contribute for this variation: (i) wave passage effect, due to finite propagation velocity; (ii) incoherence effect, due to differences in superposition of waves; and (iii) the local site amplification due to spatial variation in geological conditions. This paper discusses the procedures to be undertaken in the time domain analysis of a cable-stayed bridge under spatial variability of earthquake ground motion. The artificial synthesis of correlated displacements series that simulate the earthquake load is discussed first. Next, it is described the 3D model of the International Guadiana Bridge used for running tests with seismic analysis. A comparison of the effects produced by seismic waves with different apparent propagation velocities and different geological conditions is undertaken. The results in this study show that the differences between the analysis with and without spatial variability of earthquake ground motion can be important for some displacements and internal forces, especially those influenced by symmetric modes.

Keywords: spatial variability of earthquake ground motion; cable-stayed bridges; baseline correction.

1. Introduction

The earthquake analysis for current structures assumes a rigid base, with no consideration of spatial variability. However, when the horizontal dimension is large (typically of about 100 m or more) the codes of practice such as the Portuguese code (RSA 1984) or the Eurocode 8 (2003), state that it is no longer acceptable the assumption of the same seismic input in all foundations. The justification is clearly identified by the measures in seismographic array in Lotung, Taiwan, and by the studies of many authors (Hao 1989, Harichandran 1991, Boissières 1995, Laouami 2001).

The spatial variability of earthquake ground motion (referred to as SVEGM in this paper, for the sake of simplicity) is a consequence of three main causes: (i) the wave passage effect; (ii) the incoherence effect; and (iii) the local site amplification (LSA). The consideration of SVEGM results in the definition of distinct seismic loading for each support.

For the global seismic response of a structure, two contributions should be considered: the pseudo-static component, due to the kinematics loading, and the dynamic component, due to inertia

[†] MSc and Assistant, E-mail: ferreira@dec.uc.pt

[‡] Assistant Professor, Corresponding author, E-mail: jhnegrao@dec.uc.pt

forces. The former originates internal forces, whose influence on the overall response depends on the conception and stiffness of the structure. As the final result is hardly predictable, it is therefore necessary to evaluate the influence of SVEGM for each situation.

The analysis of a structure due to a random phenomenon is often performed by stochastic processes and evaluated in the frequency domain (Harichandran 1996, Hao 1998, Soyluk 2000), but the seismic analysis in the time domain is an attractive alternative, because of the large amount of information that it provides on the behaviour of the structure submitted to a dynamic load and of the simpler extension of the analysis algorithm for nonlinear analysis. The main disadvantage is the time required to make a statistical analysis, because the time domain approach allows only for one time history at a time. The evaluation for many time series is thus required, in order to get statistically meaningful results. This approach was nevertheless used in this work.

The direct time integration of the equilibrium equations requires the load definition in the time domain and so a procedure to synthesize the displacements, according to the spatial variation for the specific case, is needed. The correlation is normally defined in the frequency domain by coherency functions, see Harichandran (1986), Luco and Wong (1986) or Der Kiureghian (1996), but its use has an inherent difficulty on establishing the values for the parameters. In this work, only values defined in the codes of practice were used and so a simple model for accounting the SVEGM was developed. The artificial displacements are compatible with a given response spectrum.

For the evaluation of SVEGM effect, a finite-element model of the International Gadiana Bridge (Portugal-Spain southern border) is subjected to different apparent velocities and local site amplification. The results are presented.

2. Synthesis of imposed displacements

The use of a direct step-by-step method for the integration of the equilibrium equations, concerning the analysis of the SVEGM, requires a kinematics load definition. The structural analysis is thus based in time-varying displacements imposed to the supports of the structure.

In order to get those artificial records, it is recommendable to start with the generation of accelerations (Ferreira 2004), according to the following sequence: (i) estimation of the power spectral density (PSD) function; (ii) artificial generation of a pseudo-acceleration by a stationary record related to the PSD function; (iii) based on this pseudo-acceleration record, evaluation of the displacement record, through three transformations: (iv) multiplication by an intensity function, (v) baseline correction and (vi) integration.

2.1 Artificial generation

The estimation of the PSD function is made through an iterative process. First of all, a group of accelerations based on a tentative shape of the PSD function is synthesized. Then, the corresponding average response spectrum is evaluated and, from the comparison of this spectrum with that proposed by the code of practice, the PSD function is corrected (Clough and Penzien 1993). The whole process is repeated until the response spectrum is achieved.

The artificial generation of stationary records may be performed through the sum of periodic functions such as *cosine*, whose amplitudes should be related to the power spectral density function. This study uses a model suggested by Der Kiureghian (1996), in which time-varying amplitude is

proposed (1). This variation is simulated by assigning random amplitude to each period.

$$a(t_n) = \sum_{i=1}^M A_i(t_n) \cdot \cos(2\pi \cdot (i \cdot \Delta f) \cdot t_n + \theta_i) \tag{1}$$

In order to get a convenient modeling of a seismic record, it is necessary to simulate the limited duration of this natural phenomenon. A three-stage procedure was implemented, with a starting period of increasing excitation, followed by a stationary and finally by an excitation decay periods (Clough and Penzien 1993, Barbat 1994).

The Baseline correction method is used to remove the low frequency harmoniums, present in the acceleration record. These will be amplified in the integration process, in spite of being physically meaningless. For lower frequencies the displacements record tends to have high period harmoniums with large amplitude.

If the average (infinity period) of an acceleration record is not null, the shape of the displacement record will follow a parabolic pattern. It is thus necessary to remove the long period harmoniums in order to get a more realistic displacement record. This correction is more relevant for sites away from the epicenter because there are not permanent displacements induced by the earthquake. This is physically expressed by a null average velocity. The baseline correction can be evaluated through different models such as those proposed by Barbat (1994), Trifunac (1970) and Guan (2004). The first two were used in this study.

The next step required for the synthesis of a displacement record is the integration of the accelerations. One simple approach is based on the assumption of a linear variation of the acceleration between two consecutive time steps, leading to an integration scheme similar to that used in the method of Newmark. An additional requirement consists of imposing a null average velocity. An alternative procedure for this step is the Fourier Integration, which is a good method for digital signal processing because the harmoniums are well integrated. This procedure requires the correction of the displacement record through the addition of a constant. A null initial value is considered.

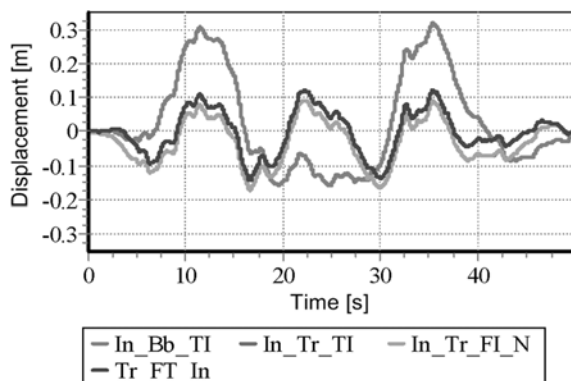


Fig. 1 Artificial displacements

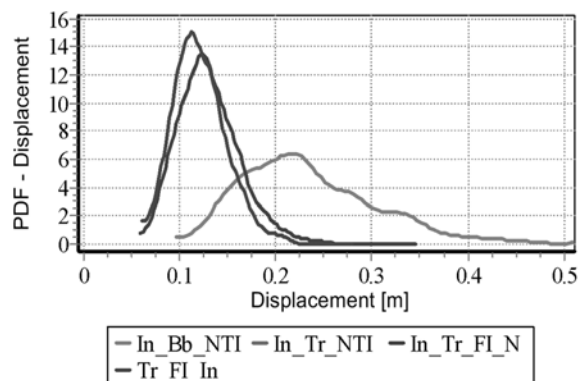


Fig. 2 PDF of maxima displacement

2.2 Displacement records

One important issue to be understood is the influence of the evaluation sequence of these processes in the synthesis of the displacements records. The sequence required to convert an acceleration record into a displacement record is not unique and may thus be modified. This change influences the final result and it is thus important to know how to use those procedures.

Fig. 1 displays four displacements records, obtained from the same stationary acceleration record by using different transformation sequences. The used nomenclature is : *In* – Intensity Function; *Bb* – Barbat Baseline Correction; *Tr* – Trifunac Baseline Correction; *TI* – Time Integration; *FI* – Fourier Integration; *N* – Make initial value null; *PDF* – Smooth probability density function. The Fig. 2 is a representation of a smooth probability density function evaluated on 1000 different records.

Figs. 1 and 2 clearly show that the baseline correction method is the most influencing process in the final result because of the long period harmoniums present in the records. The method proposed by Barbat (1994) removes only one harmonium with a period of about twice the record duration, which is not enough, especially for long time records. Consequently, the use of the Trifunac Baseline Correction method is preferred.

The numerical integration scheme does not affect the results, as shown in Figs. 1 and 2. The *In_Tr_TI* and *In_Tr_FI_N* records are overlapped.

The sequence *Tr_FI_In* has not a good physical meaning because of the artificial displacement modulation. Peaks arise for the resulting acceleration at the transition instants between stages of the modulation function – initial to stationary and stationary to final decay stages – which are meaningless. However, this sequence leads to good displacement records with a null average displacement, null initial velocity and the average maximum closer to the others, see Fig. 2.

The Trifunac baseline correction method requires the prescription of a value for cutting-off harmoniums. His proposal of the value of 16s for the cut-off period is essentially a consequence of the equipment and the accuracy of the digitalizing process.

In artificial generation, that limit can be different. In order to analyse the influence of this value, the smooth probability density functions for the maximums of 1000 displacement records were calculated and are shown in Fig. 3. The choice for the cut-off periods is based on the total record length, *Tr*, and thus the baseline correction was evaluated with $Tr = 50s$, $Tr/2 = 25s$; 16s; $Tr/4$

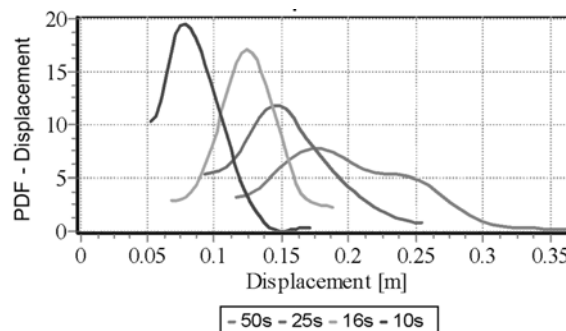


Fig. 3 PDF of maxima earthquake displacement synthesis with Trifunac baseline correction using different periods cut-off

= 12.5s and $T_r = 10$ s. The results for cut-off periods of 12.5s and 16s were nearly the same and so only the latter is shown, that is, the reference value proposed by Trifunac (1970).

The results evaluated with the value of 16s present a well defined probability density function, similar to that of the Gaussian distribution. Therefore that value was adopted. Calculations with other time durations were also performed and its comparison shows that 16s is adequate.

This cut-off period is similar to the one proposed by Guan (2004). This author presents another method for correction of the acceleration and concludes that the cut-off period of 15s normally corresponds to the best displacement response spectrum.

3. Spatial variability of earthquake ground motion

The causes of the SVEGM are not easily evaluated and some simplifications must thus be assumed. The energy loss of the seismic waves (attenuation effect), while travelling between the supports of the bridge, may be neglected, because the size of the structure is very small in comparison with the overall dimension of the earthquake event. It is also assumed that the propagation is made essentially through the bedrock, due to its high velocity, and the waves cross the layer soils by shear waves. Another simplification is the assumption that the superposition of the waves does not significantly change in different positions, which is to say that the displacements in the supports are generated by the same wave composition throughout the structure. Therefore, the differences between the displacements in bedrock are originated by the finite velocity of the waves and, as a result, the PSD function may be the same. Consequently, the incoherent effect is not used. Nazmy (1992) uses a similar approach in a part of his study. Zerva (1990) and Hao (1991) conclude that the response of very flexible structures is mostly controlled by the wave passage effect, making acceptable the simplification on neglecting the incoherence effect. The soil was considered to be made up of a number of elastic and homogeneous layers.

The model of SVEGM for simulating correlated time series in time domain considered only two causes for the spatial variability: (i) wave passage effect, due to finite apparent propagation velocity; and (ii) the local site amplification due to spatial variation in geological conditions.

3.1 Model description

In accordance to the assumptions previously referred, the implemented model considers that the seismic waves travel through the bedrock and reach the foundation level as shear waves propagating vertically. This behaviour is also assumed by Dowrick (1977).

An important issue in the characterization of the SVEGM is the propagation velocity. For the sake of simplicity, it is assumed that all types of waves have the same apparent velocity and follow a straight path, regardless its frequency (Der Kiureghian 1996). The seismic apparent velocity is thus a mean value and the time delay between the arrivals of the earthquake at different supports is easily evaluated, dividing the distance by the average apparent velocity.

The direction of the propagation is another important issue to take into consideration. As the wave delay depends on the distance between supports, the propagation in the longitudinal direction will produce more changes with respect to the rigid-base approach. For this reason, this was assumed as the travelling direction of the waves.

The local site amplification (LSA) effect also plays a fundamental role in the seismic response. In

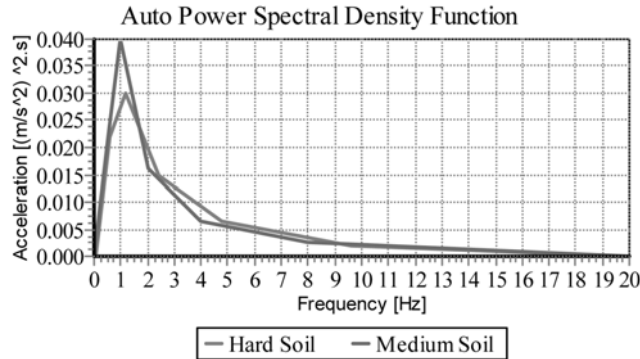


Fig. 4 PSD functions from Portuguese Code RSA

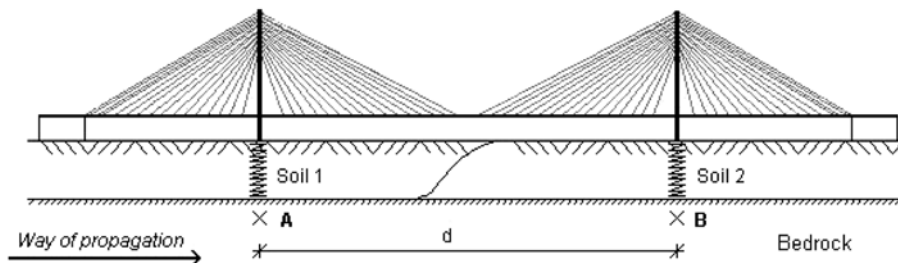


Fig. 5 Model for spatial variability of earthquake ground motion

order to define it, a shear building transfer model was considered, in which the bedrock vibration propagates as shear waves in the overlaying layers with resonant frequencies, Eq. (2), that amplify the seismic record.

$$f_k = \frac{k \cdot v_s}{4 \cdot h} \quad k = 1, 3, 5, \dots \quad (2)$$

Those frequencies depend on the layer thickness h , and on the speed of the shear waves v_s , see Safak (1995).

This effect has two contributions: a delay due to different shear velocities in different soils profile, and the change in PSD function of the frequency content and amplitudes. The former is clearly identified in Der Kiureghian (1996) coherence model, while the latter is a consequence of the filtering soil.

The examples shown in this paper use the two types of soils (Hard and medium soil) defined in RSA (1984), and they are presented in Fig. 4. This code of practice provides both the response spectra and the power spectral density functions used in this work. The differences between them result from the different frequency band of the soil filtering.

The model used for SVEGM in this study is illustrated in Fig. 5. Each support can have a different definition for the soil properties. Considering foundation soils with distinct shear velocities, different frequency ranges will be filtered as a consequence.

3.2 Calculation procedure

Regarding Fig. 5, it is assumed that the seismic waves travel from A to B. The first step consists of generating a displacement record, which will be taken as the basis for the artificial seismic load. This generation is based on the PSD function, which characterises the earthquake in the bedrock. The resulting random record is assigned to point A. Once this record is available, it is a straightforward task to estimate the records for the remaining supports, based on the assumed wave apparent velocity and on the distance between A and each of these points. These records must then be filtered, in order to simulate the propagation throughout the foundation layer.

$$u_i(t) = LSA_i \left(u_A \left(t - \frac{d_{A,i}}{V_{app}} \right) \right) \quad (3)$$

The transfer model (LSA_i) in the time domain, used in this step, is described by Safak (1995). That function is defined by 3 parameters r , τ and Q , which depend on the velocity of the shear waves, the unit mass of the rock (v_r , ρ_r) and soil (v_s , ρ_s) layers, the soil layer height h and the damping quality factor, Q . That author presents the transfer model as defined in the frequency domain and as a time recursive filter. The second choice was adopted in this study.

The parameters r and τ of the transfer models are estimated by comparison of the soil PSD function with the bedrock PSD function, in the frequency domain, knowing that

$$PSD_{soil} = |LSA(f)|^2 \cdot PSD_{rock} \quad (4)$$

The quality factor must be adopted according to literature recommendations. See Bowles (1996) or Mari (1999) as examples.

4. Seismic analysis of a cable-stayed bridge

4.1 Model description

A 3D Finite Element (FE) model based in the International Guedes River Bridge (Portugal-Spain border in Algarve) was used for the numerical test. This is a symmetric cable-stayed bridge with a total span of 666 m and a main (central) span of 324 m, see Fig. 6. The deck is 20 m above the average water level.

The grade of the concrete is C40/45 according to Eurocode 2 (2004) for the towers and for the deck. The bridge has 64 stay-cables with even spacings of 9.0 m and 1.8 m between anchorages, in

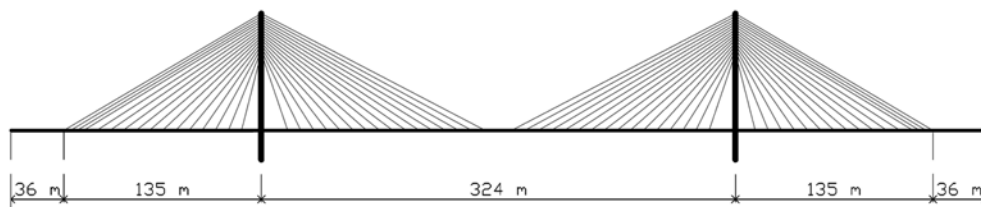


Fig. 6 Bridge model

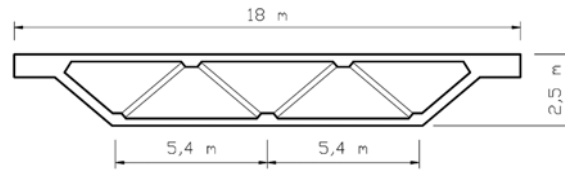


Fig. 7 Transversal deck section

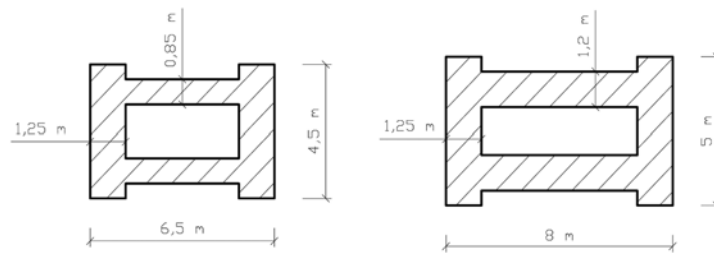


Fig. 8 Tower sections

the deck and in the towers, respectively. The deck is also supported by the towers with a hinged link.

The deck section is a single box with 2.5 m tall and a width of 18 m. The thickness of the upper and lower plate is 0.25 m and the inclined walls have a thickness of 0.35 m. At every 4.5 m the section is reinforced by a metallic truss composed by hollow elements of $200 \times 200 \times 6.5$ mm. The side cantilevers are enlarged in order to ensure a well distributed stress due to the forces induced by the stay-cables, see Fig. 7.

The deck is modeled with two longitudinal stiffening girders and evenly spaced transverse girders. The Euler-Bernoulli formulation was used and the geometric characteristics of the beam elements were set in order to get the same longitudinal and transversal bending inertia, area, torsional and distortional stiffness as those computed by modeling the deck with shell elements. The considered value of the mass was such that the main frequencies resulted close to those obtained with the actual box-girder geometry.

The inverted Y towers have a total height of 100 m. The sections of the lower and upper part of the towers are represented in Fig. 8, respectively on the left and on the right.

The dynamic behaviour of a cable-stayed bridge is strongly affected by the deck-to-pylon and deck-to-abutment connections. In this model, no longitudinal connection was considered. With such structural system, the first vibration mode has an important contribution for the overall bridge response. The evaluation of the frequencies is performed and the results for the most relevant longitudinal (anti-symmetric) and vertical (symmetric) modes are presented in Fig. 9.

4.2 Analysis

The effects under control are the longitudinal displacement at the top of the left tower (referred to as *tower top*), the longitudinal displacement and the axial force in the deck middle section (*deck*) and the shear force and bending moment at left tower base (*tower base*). The presented results are the average of the maximum of 50 different time-series.

The average apparent propagation velocity has an important role in the seismic analysis, since the

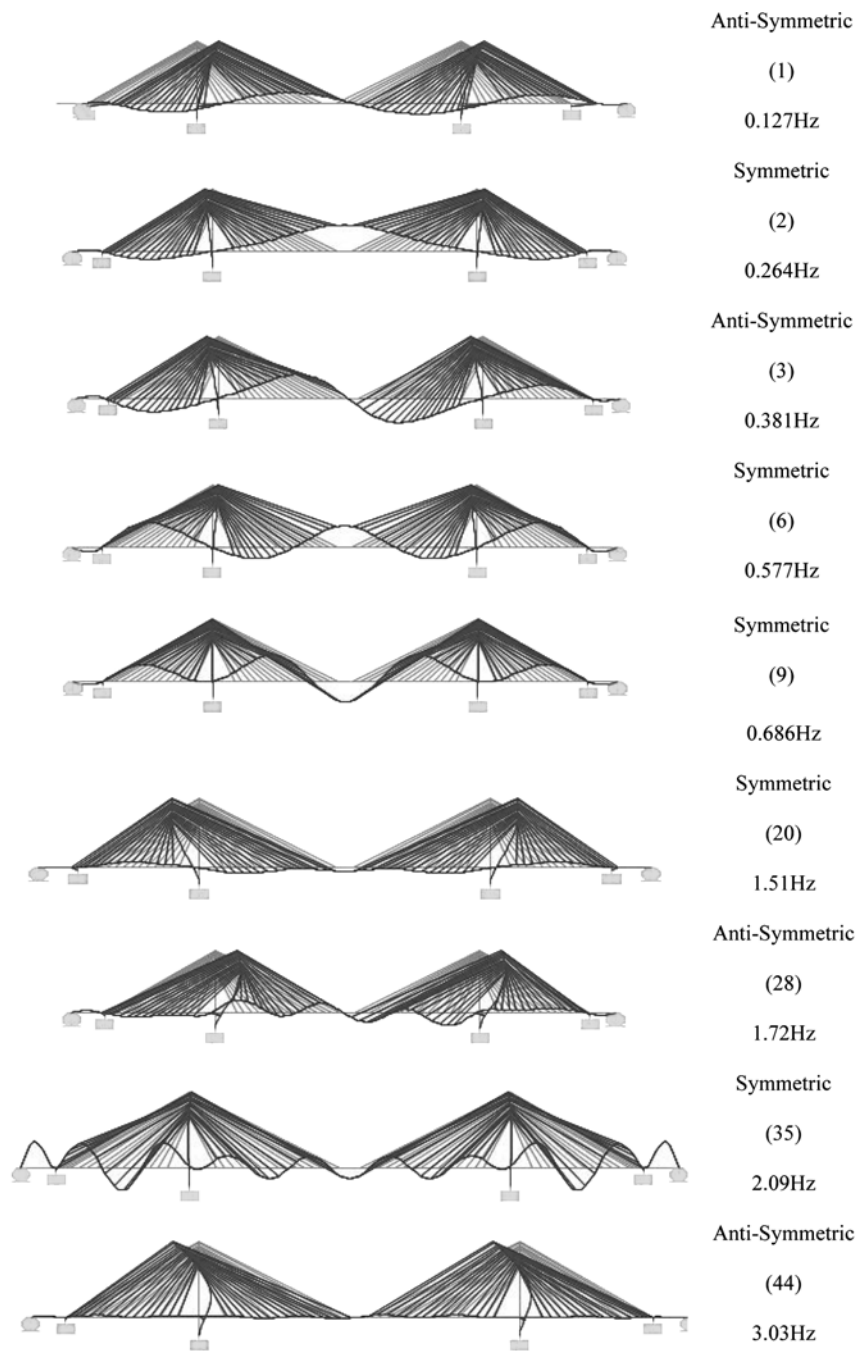


Fig. 9 Vibration modes

wave passage effect depends directly from this value. In the references there are many values, so the chosen value of 2000 m/s reflects an average apparent velocity (Harichandran 1996, Laouami 2001, Zanardo 2002).

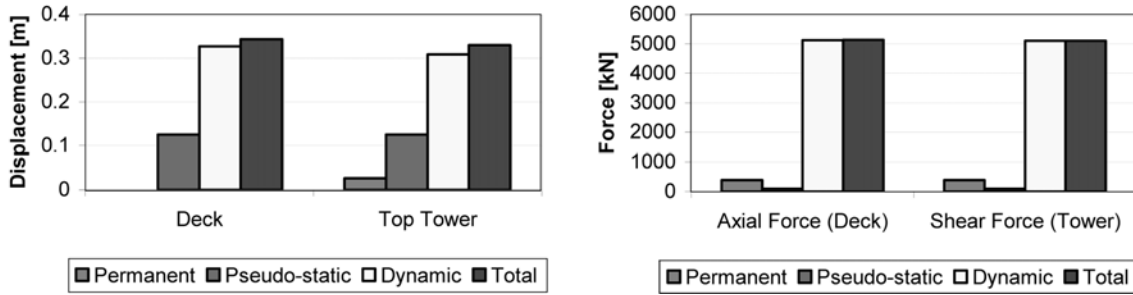


Fig. 10 Bridge response

4.2.1 Contribution of the pseudo-static component

In a multi-support excitation there are two components that influence the seismic response: pseudo-static and dynamic component. These two components with the contribution of permanent load and the total seismic response are shown in Fig. 10. The results are evaluated assuming an apparent velocity of 2000 m/s and without local site amplification.

The results presented in these graphics show that the pseudo-static component has an insignificant contribution for overall earthquake response, but its influence is visible in a lower dynamic displacements response.

4.2.2 Excited modes due to SVEGM

The rigid base earthquake is an anti-symmetric loading, only exciting the corresponding vibration modes. The consideration of the SVEGM adds a symmetric component to the response, which is

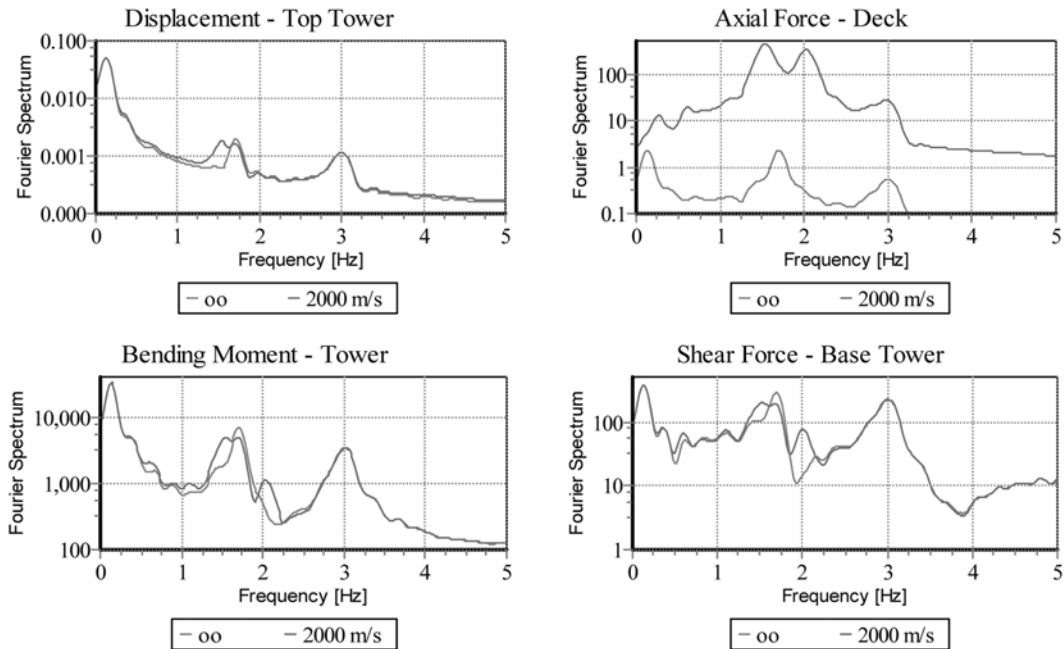


Fig. 11 Fourier spectra for bridge response

not thus predictable.

With the purpose of illustrating this conclusion, Fig. 11 shows the Fourier spectra of the responses with an infinite velocity and an apparent propagation velocity of 2000 m/s.

These results allow some conclusions to be drawn: (i) the importance of the first anti-symmetric modes, once that all responses show a peak near the corresponding frequency; (ii) when a finite apparent velocity is considered, the symmetric modes with a frequencies about 1.5 Hz and 2 Hz are excited; (iii) the axial force on the deck is substantially increased with SVEGM.

5. Results

In this section, the results for different apparent propagation velocities and the influence of the local site amplification are presented.

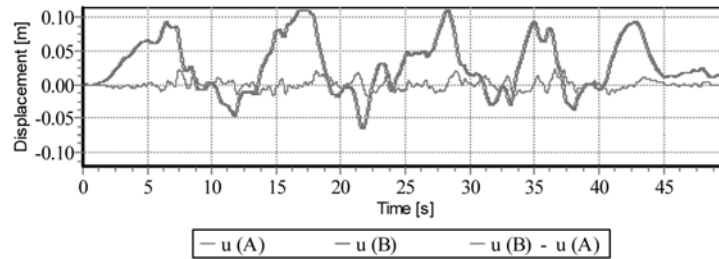


Fig. 12 Example of one input

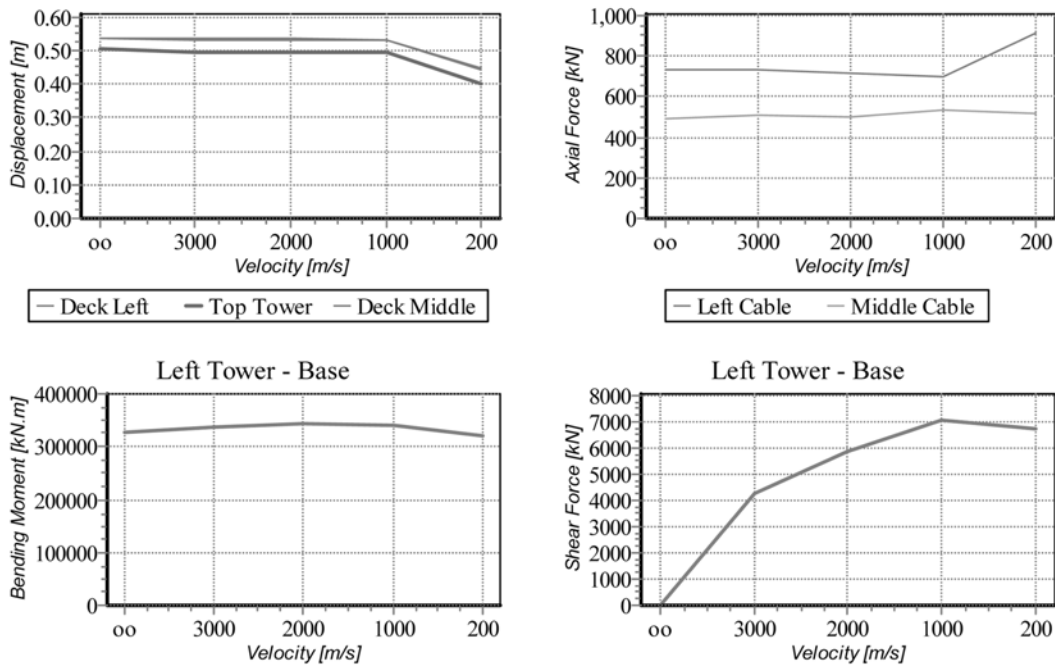


Fig. 13 Seismic responses due to wave passage effect

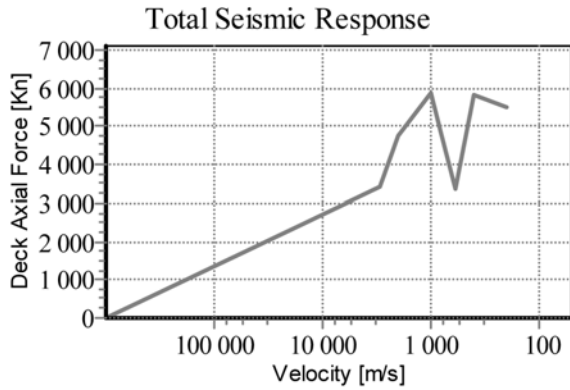


Fig. 14 Variation of deck axial force due to wave passage effect

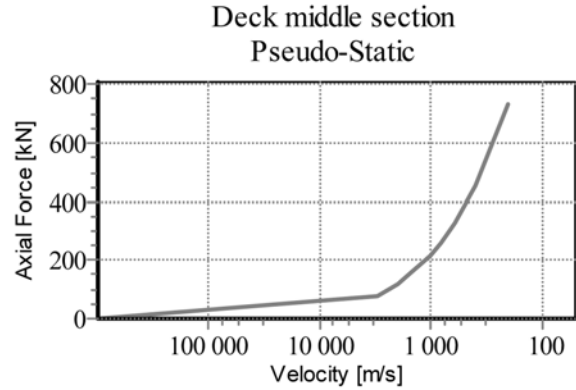


Fig. 15 Evolution of the pseudo-static component due to wave passage effect

The method of Newmark with average acceleration was used for the numerical solution of the dynamic equilibrium equation, with a Rayleigh damping model with a 2% coefficient damping associated to the frequencies 0.5 Hz and 3 Hz.

The seismic load used in these examples refers to a type-2 earthquake (strong earthquake with large focus distance), with a 30s duration in stationary part, as defined in RSA (1984), see Fig. 4. The near field earthquake was not considered, because preliminary tests have shown that its effects, in the present structure, were clearly lower than those of far field earthquake. The Fig. 12 represents one example of the inputs and the difference between them. The apparent velocity used is 2000 m/s.

In order to evaluate the effect of spatial variability, the responses of the bridge for apparent propagation velocities of ∞ , 3000 m/s, 2000 m/s and 1000 m/s, were evaluated. The wave apparent velocity of 200 m/s is used to put in evidence the trend of the spatial variability effect.

The values presented are the average of 50 different displacement series.

From Fig. 13 it is possible to conclude that lower apparent velocity results in lower displacement. The justification is the reduction of dynamic component.

The axial force in the deck middle section is strongly increased with the reduction of the apparent propagation velocity. This effect is a consequence of the excitation of the symmetric modes, caused by the symmetric part of the instantaneous displacements in the supports. However and unexpectedly, a decrease was noticed for the case of the wave velocity of 200 m/s. In order to investigate the reason for that, the additional cases of 800 m/s, 600 m/s and 400 m/s were studied. The results are the average of 20 different time-series, as shown in Figs. 14 and 15.

By analysing Fig. 15, it is possible to conclude that the pseudo-static effect is very small when compared with the global seismic response, and does not explain the local minimum at 600 m/s. This apparent propagation velocity causes a wave delay of 0.54s in a distance between supports of 324 m, which is closer to the period of some symmetric modes. Therefore those modes are weakly excited and as a consequence the earthquake response is lower, Fig. 16.

For the investigation of the local site amplification effect, the average maximum of 50 responses of a series of two input displacement records calculated by the rules presented above, were computed. The displacement in point A is always the same, while for point B it was evaluated for the different cases. The results are presented in Table 1.

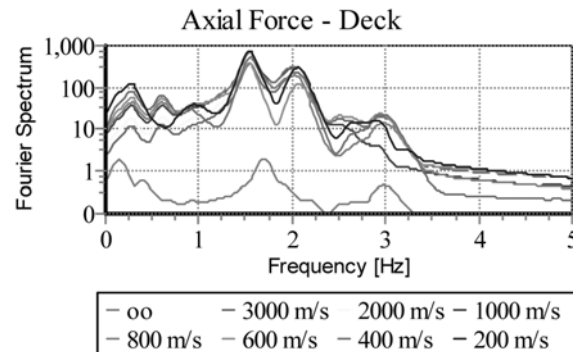


Fig. 16 Fourier spectrum for axial force due to wave passage effect

Table 1 SVEGM response for wave passage and local site amplification

		Wave passage only		Wave passage and local site amplification	
Velocity		∞	2000 m/s	∞	2000 m/s
Displacements	Top Tower	0.5039 m	0.4944 m	0.4988 m	0.4950 m
	Left Deck	0.5353 m	0.5326 m	0.5325 m	0.5283 m
	Middle Deck	0.6265 m	0.6251 m	0.6260 m	0.6217 m
Cables	Left	730.8 kN	716.0 kN	708.4 kN	699.4 kN
	Middle	495.7 kN	503.0 kN	535.5 kN	557.3 kN
Left Tower Base	Shear Force at Tower Base	6332 kN	6540 kN	6237 kN	5835 kN
	Bending moment	328.1 MN.m	342.6 MN.m	343.0 MN.m	337.2 MN.m
Deck	Axial Force - Middle	31.70 kN	5888 kN	7349 kN	5844 kN

The PSD functions used for the numerical examples are quite similar. Therefore, the local site amplification is only evidenced by the first factor, the shift phase (Der Kiureghian 1996, Safak 1995). This effect is similar to the wave passage.

6. Conclusions

In order to undertake the seismic analysis of a structure to be erected in a region with scarce data from actual earthquakes, a possible alternative is the use of artificial records, generated in accordance to the requirements of codes of practice. In this paper, issues concerning the procedures involved in the generation of such imposed displacements were discussed. Some attention was also paid to the procedure to account for the spatial variability of the earthquake ground motion. This issue is of some relevance in long structures such as suspended or cable-stayed bridges, or when different soil conditions exist in the different supports.

The longitudinal displacements are smaller when the spatial variability of earthquake ground

motion is considered. The internal forces show an opposite trend. The values of the bending moment and the shear force at the left tower, evaluated with SVEGM, are 3% and 4% higher than those obtained by using the rigid base approach. The axial force in the deck, which is essentially controlled by the symmetric modes, is extremely increased with spatial variation. This internal force shows that the value of the wave delay plays an important role on the SVEGM response due to the symmetric modes.

Differently from expected, the study does not reveal a clear trend for the local site amplification (LSA) effect, but this may be due to the PSD functions provided by RSA, which show quite similar frequency contents for different soil profiles. Therefore, a careful analysis is required when significant differences in geological conditions exist between the foundations of the bridge. Another consequence of the consideration of LSA, also highlighted by this study, is the time delay due to a relative lower shear velocity.

References

- Barbat, A. and Canet, J. (1994), *Estructuras Sometidas a Acciones Sísmicas*. 2ª edición. CIMNE. Barcelona.
- Boissières, H.P. and Vanmarcke, E.H. (1995), "Estimation of lags for a seismograph array – Wave propagation and composite correlation", *Soil Dyn. Earthq. Eng.*, **14**(1), 5-22.
- Bowles, J. (1996), *Foundation Analysis and Design*. Fifth edition, McGraw-Hill International Editions, Singapore.
- Clough, R. and Penzien, J. (1993), *Dynamics of Structures*, Second edition, McGraw-Hill, Singapore.
- Dowrick, D. (1977), *Earthquake Resistant Design*, John Wiley & Sons.
- Eurocode 2 (2004), EN 1992-1-1 Eurocode 2: Design of concrete structures. Part1-1: General rules and rules for buildings, CEN.
- Eurocode 8 (2003), prEN 1998-2 Final PT Draft (Stage 34) Eurocode 8: Design of structures for earthquake resistance. Part2: Bridges, CEN.
- Fernandes, J.A. and Santos, L.O. (1993), *Pontes atirantadas do Guadiana e do Arade*, LNEC, Lisboa
- Ferreira, M. and Negrão, J. (2004), "Spatial variation of ground motion: Synthesis of correlated displacements", *Proc. of the Seventh Int. Conf. on Computational Structures Technology*, Lisbon.
- Guan, J., Hao, H. and Yong, L. (2004), "Generation of probabilist displacement response spectra for displacement-based design", *Soil Dyn. Earthq. Eng.*, **24**(2), 149-166.
- Hao, H., Oliveira, C.S. and Penzien, J. (1989), "Multiple-station ground motion processing and simulation based on SMART-1 array data", *Nucl. Eng. Des.*, **121**(11), 1557-1564.
- Hao, H. (1991), "Response of multiply supported rigid plate to spatially correlated seismic excitations", *Earthq. Eng. Struct. Dyn.*, **20**(9), 821-838.
- Hao, H. (1998), "A parametric study of required seating length for bridge decks during earthquake", *Earthq. Eng. Struct. Dyn.*, **27**(1), 91-103.
- Harichandran, R.S. and Vanmarcke, E.H. (1986), "Stochastic variation of earthquake ground motion in space and time", *J. Eng. Mech.*, ASCE, **112**(2), 154-174.
- Harichandran, R.S. (1991), "Estimating the spatial variation of earthquake ground motion from dense array recordings", *Struct. Saf.*, **10**, 213-233.
- Harichandran, R.S., Hawwari, A. and Sweidan, B.N. (1996), "Response of long-span bridges to spatially varying ground motions", *J. Struct. Eng.*, ASCE, **122**(5), 476-484.
- Der Kiureghian, A. (1996), "A coherency model for spatially varying ground motions", *Earthq. Eng. Struct. Dyn.*, **25**(11), 99-111.
- Laouami, N. and Labbe, P. (2001), "Analytical approach for evaluation of the seismic ground motion coherency function", *Soil Dyn. Earthq. Eng.*, **21**(8), 727-733.
- Luco, J.E. and Wong, H.L. (1986), "Response of a rigid foundation to a spatially random ground motion", *Earthq. Eng. Struct. Dyn.*, **14**(6), 891-908.

- Mari, J., Glangeaud, F. and Coppens, F. (1999), *Signal Processing for Geologists and Geophysicists*, Éditions Technip, France.
- Nazmy, A. and Abdel-Ghaffar, A. (1992), "Effects of ground motion spatial variability on the response of cable-stayed bridges", *Earthq. Eng. Struct. Dyn.*, **21**(1), 1-20.
- RSA (1984), *Regulamento de Segurança e Acções para Estruturas de Edifícios e Pontes*. Imprensa Nacional Casa da Moeda. Lisboa.
- Safak, E. (1995), "Discrete time analysis of seismic site amplification", *J. Eng. Mech.*, ASCE, **121**(7), 801-909.
- Soyluk, K. and Dumaglu, A.A. (2000), "Comparison of asynchronous and stochastic dynamic responses of a cable-stayed bridge", *Eng. Struct.*, **22**(5), 435-445.
- Trifunac, M. (1970), "Low frequency digitalization errors and a new method for zero baseline correction of strong-motion accelerograms", Report No. EERL 70-07. Pasadena – California.
- Zanardo, G, Hao, H. and Modena, C. (2002), "Seismic response of multi-span simply supported bridges to a spatially varying earthquake ground motion", *Earthq. Eng. Struct. Dyn.*, **31**(6), 1325-1345.
- Zerva, A. (1990), "Response of multi-span beams to spatially incoherent seismic ground motions", *Earthq. Eng. Struct. Dyn.*, **19**(6), 819-832.